International Journal of Environmental Monitoring and Analysis
2016; 4(3): 94-101
http://www.sciencepublishinggroup.com/j/ijema
doi: 10.11648/j.ijema.20160403.15
ISSN: 2328-7659 (Print); ISSN: 2328-7667 (Online)

Spatial and Temporal Variations of Aerosol Optical Depth and Influence Factors over the East China Sea

Xiao-shen Zheng, Ya-nan Zhang, Yue Pan

Tianjin Key Laboratory of Marine Resources and Chemistry, College of Marine and Environmental Science, Tianjin University of Science and Technology, Tianjin, P. R. China

Email address:
zhengxiaoshen@163.com (Xiao-shen Zheng)

To cite this article:
Xiao-shen Zheng, Ya-nan Zhang, Yue Pan. Spatial and Temporal Variations of Aerosol Optical Depth and Influence Factors over the East China Sea. *International Journal of Environmental Monitoring and Analysis*. Vol. 4, No. 3, 2016, pp. 94-101.
doi: 10.11648/j.ijema.20160403.15

Received: April 29, 2016; **Accepted**: May 12, 2016; **Published**: May 28, 2016

Abstract: Atmospheric aerosols are solid and liquid particles suspended in the air, which has an important effect in macroscopic climate change. The aerosol optical depth (i.e, AOD) is one of the main factors to characterize the composition and the content of the aerosol. This study was conducted over the area of East China Sea (24ºN-41ºN, 117ºE-128ºE) based on the monthly average AOD data and monthly average wind data of 10 meter over sea surface during 2003-2013. The AOD distribution has the annual periodic variation, the AOD values increased significantly from January to March, and reached the maximum 0.133 in March, and the AOD values declined from April to August, and they stabilized around 0.1 in September to December. The trend of seasonal changes indicated that the AOD values were the highest in the spring, and slightly higher in the winter. The AOD values of spring and winter were significantly higher than the summer and the autumn. For time-series variation, the maximum of AOD values during certain periods gradually increase from 2003 to 2009, and the maximum of AOD values during certain periods gradually decrease from 2009 to 2013. Analyzing the relationship between spatial distribution of AOD and wind vectors over the sea surface, the spatial and temporal distribution and variation of AOD were closely related to the wind direction and speed over the East China Sea.

Keywords: Aerosol Optical Depth, Spatial and Temporal Variation, Wind, the East China Sea

1. Introduction

Atmospheric aerosols are solid and liquid particles suspended in the air. With the rapid development of industry, the combustion of fossil fuel, the emissions of industrial fumes and contaminated gas led to the significant increase of atmospheric aerosol, which not only affects the macroscopic climate, but also reduces the comfort of the living environment and threat to human health. The indirect effect of aerosols on climate occurs by modifying the optical properties (An W. J., et al. 2007; Lee S., et al. 2009; Tai A. P. K., et al. 2010). The most common parameter derived from satellite observations is the Aerosol Optical Depth (AOD), which is a measure of the extinction of electromagnetic radiation at a given wavelength due to the presence of aerosols in an atmospheric column. AOD is the key factor to calculate the content of the aerosol, evaluating the conditions of the atmosphere and the effect of atmosphere aerosol on climate. It is important for the research of haze and atmospheric correction.

In recent decades, with the development of science and technology, the theoretical knowledge of aerosol science are improved, the research on AOD has been focused on. Since the development of aerosol remote sensing in mid-1970, many AOD retrieval algorithms has been developed (Glantz P., et al. 2009, Yuan Y., et al. 2014, Li Y. J., et al. 2013). For MODerate resolution Imaging Spectroradiometer (MODIS) sensors the available algorithms of marine aerosol optical depth are single-channel reflectance method (Fraser R. S., et al. 1984, Moula M., et al. 2002,Wang J., et al. 2010) and double-multi-channel reflectance methods (Sundström A.M., et al. 2012), in which high accuracy of AOD inversion results can be obtained from the multi-channel reflectance method. However, the satellite-derived AOD is a measure of light attenuation in the column which is affected by environment

conditions. Many scholars have studied the aerosol properties, composition and distribution characteristic of the specific area (Cong Z. Y., et al. 2007, 2009, Chudnovsky A. A., et al. 2014).

The long-term trend of aerosol optical depth over the global oceans has been studied by using a nearly 25-year aerosol product from the AVHRR data. This negative tendency is even more evident for globally and annually averaged AOD with the magnitude of -0.03 /decade. The decreasing tendency in global AOD is consistent with that from the remote sensing data set (Mehta M., 2015, Meij A. de, et al. 2012). The trends in AODs, temporally and spatially was analyzed with MODIS data (2000-2008) over eight typical regions in China (Guo J. P., et al. 2011)

The East China Sea is located the western of Pacific Ocean, which is strongly affected by monsoons, massive freshwater outflows, tides and the Kuroshio (Chen C.-T. A., 2009). Therefore the study of the spatial and temporal distribution of AOD and its influence factors are significant to the national economy sustainable development and the environment protection. Aerosol retrieval using MODIS data has been well researched over the past decade (Luo N. N., et al. 2015, Lee J., et al. 2014,). This study was conducted over the area of East China Sea (24ºN~41ºN, 117ºE~128ºE) as the research area and bases on the monthly AOD data from MODIS sensor and monthly wind data of 10 meter over sea surface provided by ECMWF during 2003-2013. Then the characteristics of spatial and temporal variation of aerosol optical depth and the effects of the wind field to its distribution were analyzed.

2. Data and Methods

2.1. Study Area

The East China Sea (i.e., the Bohai, Yellow and East China Sea) is marginal sea surrounded by bordered by Kyushu and the Ryukyu Islands of Japan, Taiwan Island, mainland China, and the Korea Peninsula. The almost enclosed Bohai Sea (BS), with a surface area of 77×10^3 km^2, is the smallest and shallowest of the three seas with an average depth of only 18 m. The semi-enclosed Yellow Sea (YS) has a surface area of 380×10^3 km^2, an average depth of 44 m, it sits entirely on the continental shelf. The more open East China Sea (ECS), at 770×10^3 km^2, is the largest of the three seas, with an average depth of 370 m (Sun, X. P. 2008, Chen C.-T. A., 2009).

The study area of the East China Sea (24ºN~41ºN, 117ºE~128ºE) are shown as Fig. 1. It is characterized with high loadings of sediment concentrations in the continental shelf regions. The Yellow River, the liaohe, yalu, and Haihe, also transport significant amounts of sediment into the Bohai, Yellow and East China Sea. It is suffered from the East Asian monsoon, the ecological environment of the Yellow Sea and East China Sea has changed greatly in the past few decades.

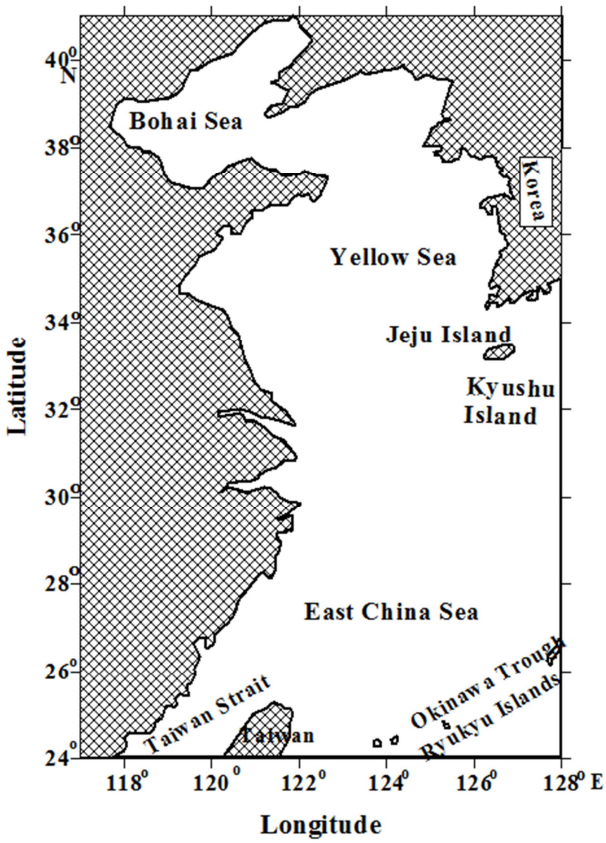

Fig. 1. *The study area- shelf of East China Sea.*

2.2. Satellite Data Collection of AOD

The standard mapped satellite images from MODIS/Aqua were used to derive the AOD values over the East China Sea. Monthly averaged climatology AOD values from January 2003 to December 2013 were used. These satellite data were obtained from the Ocean Biology Processing Group (OBPG) of the Goddard Space Flight Center (GSFC) (http://oceandata.sci.gsfc. nasa.gov/MODISA/Mapped/ Monthly/9km/aot/) in the compressed Hierarchical Data Format (HDF). The basic algorithm was used for calculating the AOD.

2.3. ERA-interim Global Reanalysis Dataset of Wind

The 10m wind field of u- and v-components of horizontal wind dataset produced by the European Centre for Medium-Range Weather Forecasts (ECMWF, http:// apps.ecmwf.int/datasets/data/interim_full_moda/) was processed. The ERA-interim global reanalysis 10m wind field provided global coverage (Stopa J. E. et al, 2014). In this paper, we used the wind dataset retrieved for the same time span from January 2003 to December 2013, and the same domain (24ºN~41ºN, 117ºE~128ºE) used for the AOD retrieval.

2.4. Statistical Methods

To analyze the significant variation periods of the long-time series, we introduced the statistical method of discrete power spectral density. The basic principle is to compute the

Fourier coefficients. For a sequence $x_t(t = 1,2,\dots n)$ with n sizes, the equations represent below (Wei. F. Y.2007).

$$a_k = \frac{2}{n}\sum_{t=1}^{n}\frac{x_t \cos 2\pi k}{n}(t-1) \quad (1)$$

$$b_k = \frac{2}{n}\sum_{t=1}^{n} x_t \sin\frac{2\pi k}{n}(t-1) \quad (2)$$

$$s_k^2 = \frac{1}{2}(a_k^2 + b_k^2) \quad (3)$$

$$T_k = \frac{n}{k} \quad k = 1,2,\dots,\left[\frac{n}{2}\right] \quad (4)$$

Where k represents wave number; t is the length of time series; s_k is the power spectral density of k; T_k is the resonance cycle of k.

In the paper, n equals to 132 representing 132 months from January 2003 to December 2013; k equals from 1to 66 (half of n).

Finally, we introduced F-inspection to inspect the resonance cycle T_k, using $1-\alpha = 0.95$ confidence limit. The F-inspection equation is:

$$F = \frac{\frac{\frac{1}{2}\left(a_k^2+b_k^2\right)}{2}}{\frac{\left(S^2-\frac{1}{2}\left(a_k^2+b_k^2\right)\right)}{(n-2-1)}} \quad (5)$$

$$S^2 = E(x^2) - [E(x)]^2 \quad (6)$$

Where 2 and n-2-1 represent the freedom of numerator and denominator respectively, S^2 is the variance of the time series. When $F \geq F_{\alpha(2,n-2-1)}$, it implies that the corresponding period was marked.

3. Results and Discussion

3.1. Seasonal and Inter-annual Variability of AOD

The monthly average of AOD values over the East China Sea are shown as Fig. 2, which is from January 2003 to December 2013. The thick line is the average AOD climatology values of same month in the eleven years, which showed that the AOD values increased significantly from January to March, and reached the maximum 0.133 in March, and the AOD values declined from April to August, and they stabilized around 0.1 in September to December. During the period from January 2003 to December 2013, the highest values of AOD existed in February or March, and the lowest values of AOD appeared in different month.

April, July, October and January are the months of spring, summer, autumn and winter. The average AOD values over the East China Sea in 11 years from 2003 to 2013 are the seasonal average of AOD values, which shown as Fig. 3. The trend of seasonal changes indicated that the AOD values were the highest in the spring, and slightly higher in the winter. The AOD values of spring and winter were significantly higher than the summer and the autumn. In the four seasons, the highest values of AOD existed in spring except for 2005. The abnormal low AOD values in spring and abnormal high AOD values in summer existed in 2005. This may be related to the unusual wind speed in 2005.

The time-series variation of AOD values from January 2003 to December 2013 over the East China Sea is shown as Fig. 4. Discrete power spectrum method was adopted to test significance of AOD anomalies. Confidence interval of 0.95 was used for the test. The results clearly demonstrated the annual cycle of AOD. The AOD values began to rise in January, and reached the maximum of AOD values in February or March or April, then gradually decreases, reaches the minimum of AOD values in November or December. For time-series variation, the maximum of AOD values during certain periods gradually increase from 2003 to 2009, and the maximum of AOD values appeared in March or April. The results show that a continual upward tendency during 2003-2009(0.0038 / decade), which is similar with the results of Guo Jianping (Guo J. P., et al. 2011). The maximum of AOD values during certain periods gradually decrease from 2009 to 2013, and the maximum of AOD values appeared in February or March. The results show that a continual downward tendency during 2009-2013(0.005 / decade).

3.2. Distribution of Spatial Variation of AOD

According to the latitude and longitude the average AOD of pixel point in the same month from 2003 to 2013, the average of AOD values were shown as the distribution of spatial variation of AOD from January to December. April, July, October and January are the months of spring, summer, autumn and winter and the AOD distribution seasonal variation shown in Fig. 5.

In spring, the average values of AOD are high over the whole study area. The AOD values over coastal waters, the new estuaries of the Yellow Sea are higher than that over the central of Bohai Sea. AOD values over the Yellow Sea area are generally high(0.12-0.14), AOD values over the whole East China Sea are high, especially the highest AOD values over Taiwan Strait and the Okinawa appears 0.16.

The average of AOD values in summer is low significantly comparing with the spring. High AOD value mainly concentrated over southwest of the central Bohai Sea. The AOD values are low over the coastal waters of Bohai Sea in summer comparing with the spring. The average AOD values over the entire Yellow Sea area are significantly lower than those in the spring and only a few remnants of the higher AOD values over the south Yellow Sea, especially over the west coast and south central Yellow Sea. AOD values over the East China Sea are low significantly comparing with the spring, especially in Taiwan Strait and the Okinawa.

In autumn, the AOD values over most of the East China Sea are low, the lowest values are around 0.03 over the northeast of Bohai Sea, and the AOD values over Yellow Sea are low, while the AOD values showed significant growth trend over most of the East China Sea, especially in the coastal water.

In winter, the AOD values over the central Bohai Sea are low, the AOD values retains 0.03 over the northeast of Bohai Sea. The AOD values over North Yellow Sea displayed a

decreasing tendency. The AOD values increase significantly comparing with the autumn over the West of the Southern Yellow Sea, while the AOD values decreased over the other regions of Yellow Sea. The AOD values over East China Sea increased continuously from autumn, especially in Okinawa Trough waters and Jeju Island.

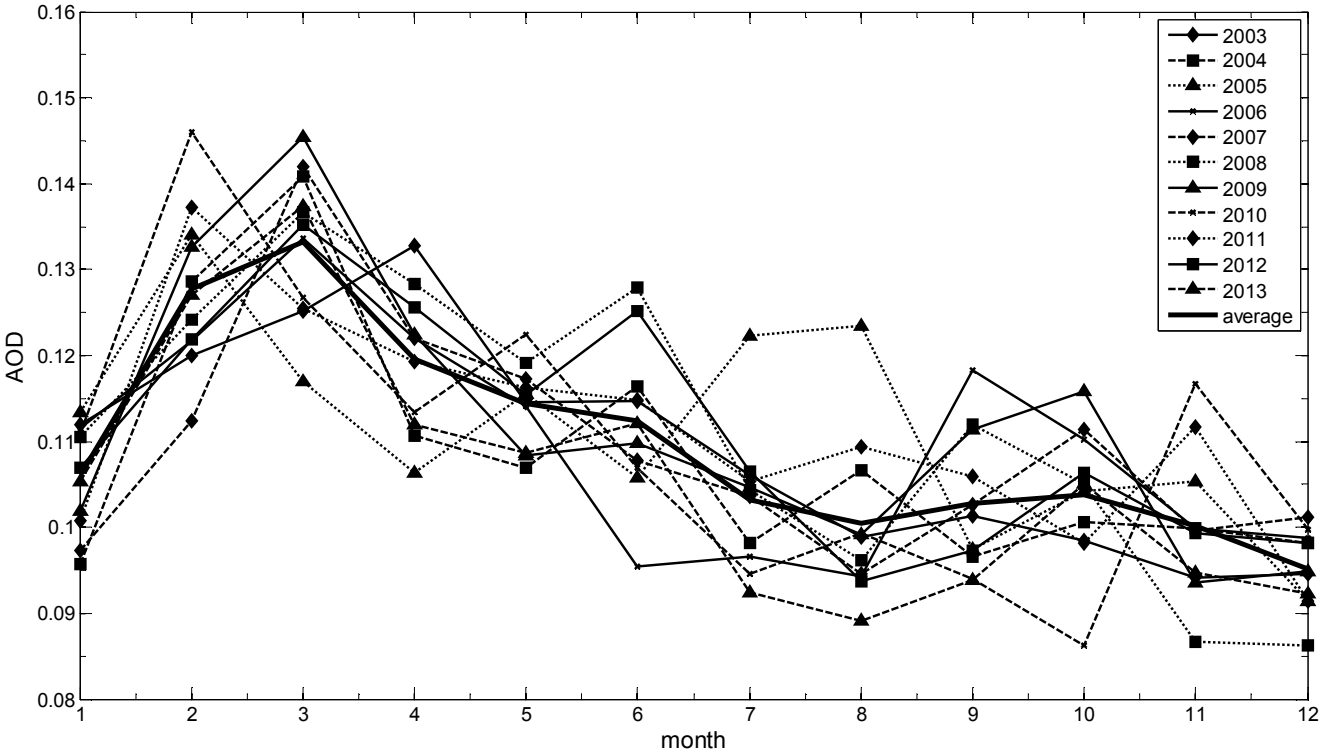

Fig. 2. *Monthly average variation of AOD from January 2003 to December 2013.*

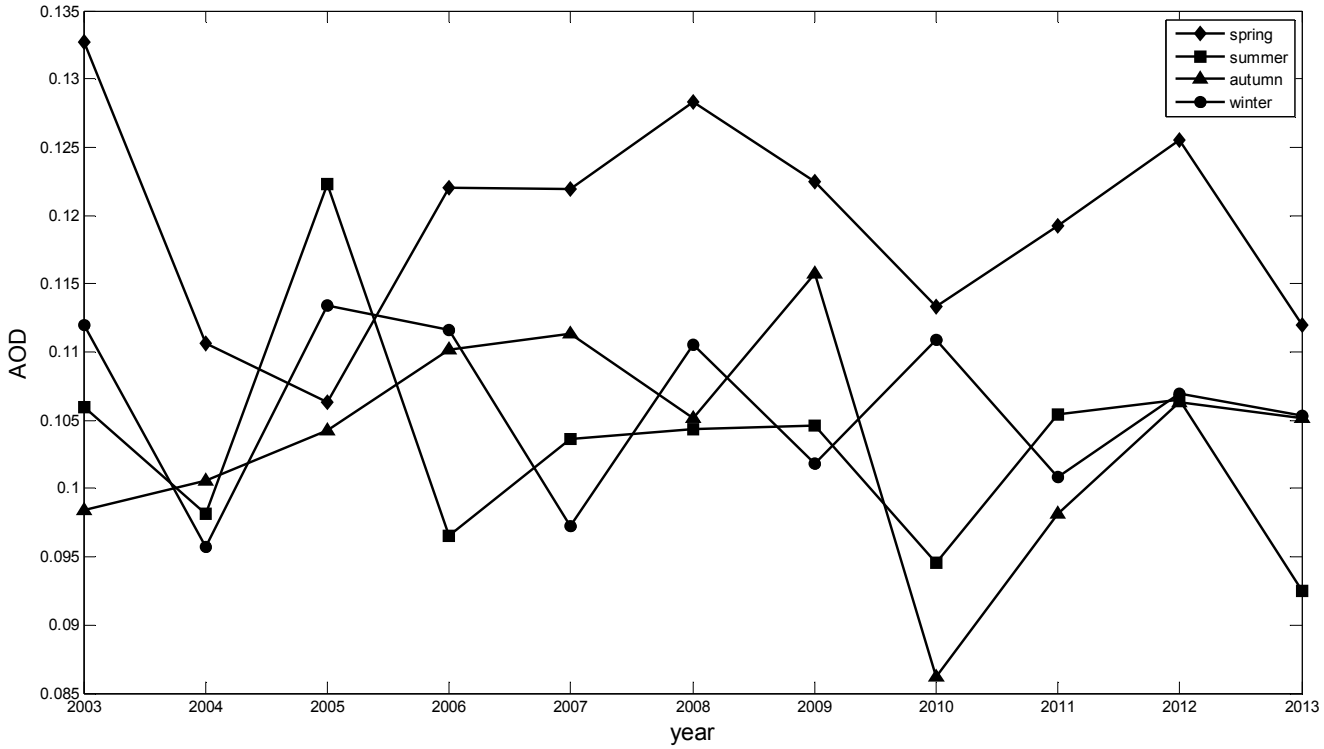

Fig. 3. *Trend of seasonal average variation of AOD from 2003 to 2013, April, July, October and January are the months of spring, summer, autumn and winter.*

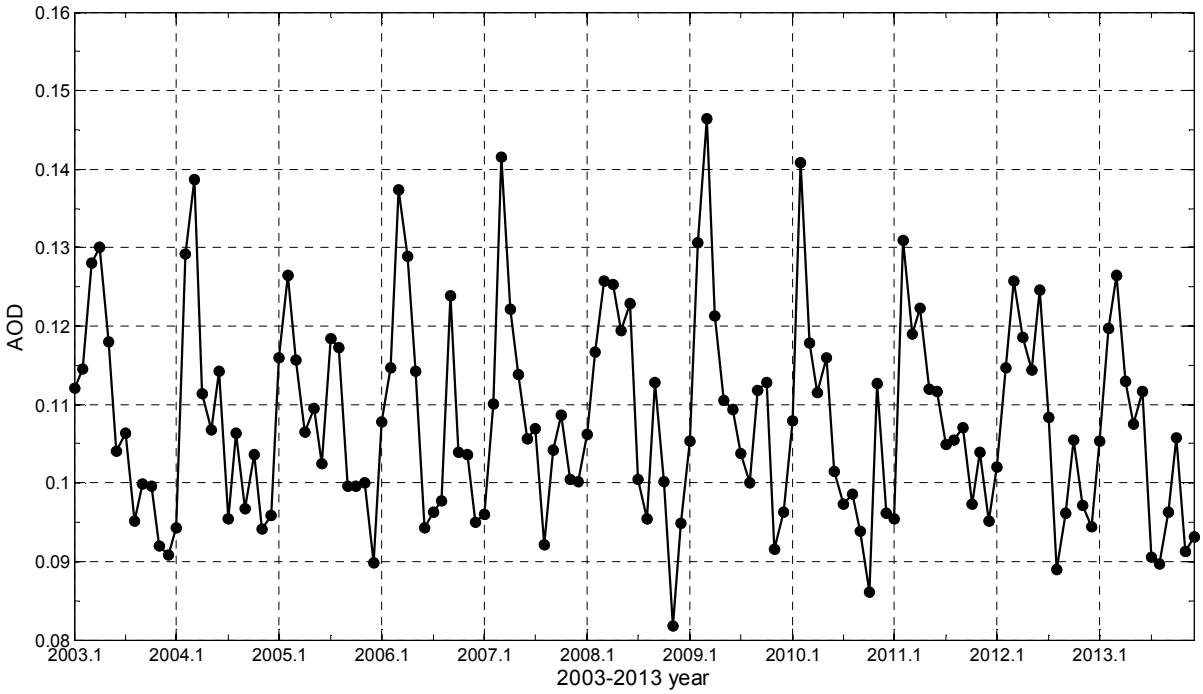

Fig. 4. *The time-series variation of AOD values January 2003 to December 2013.*

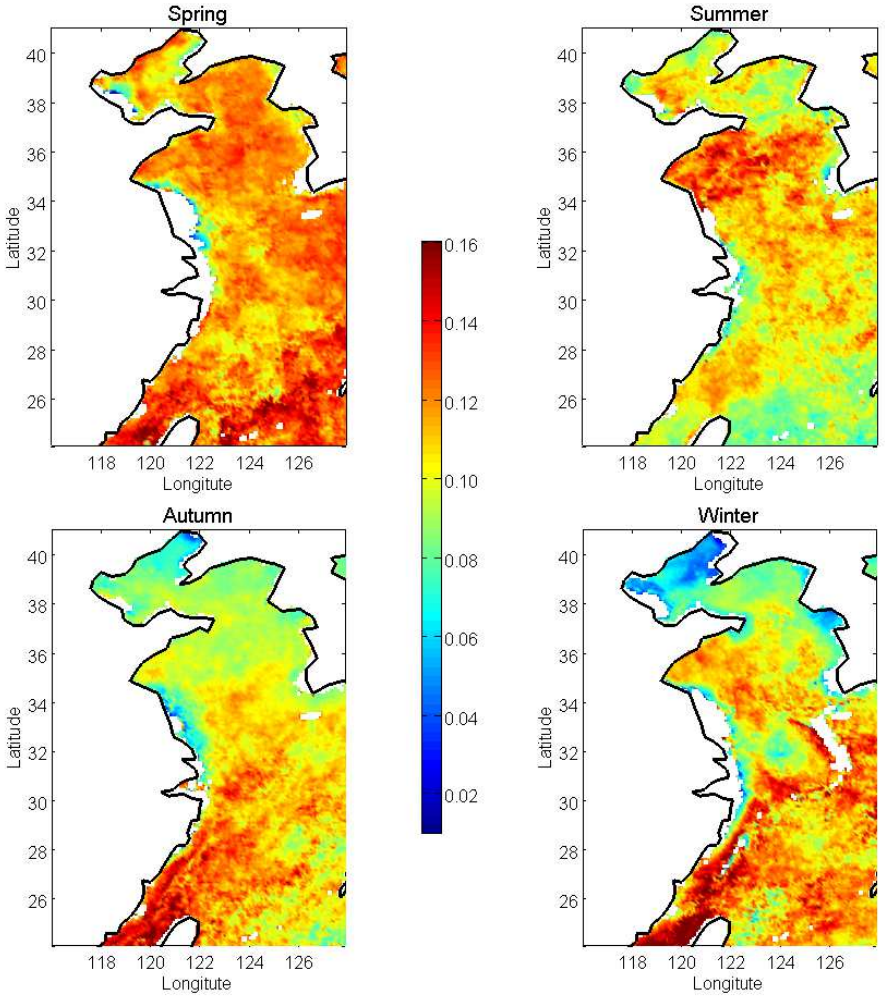

Fig. 5. *Spatial distribution of seasonally variation of AOD in 2003-2013, April, July, October and January are the months of spring, summer, autumn and winter.*

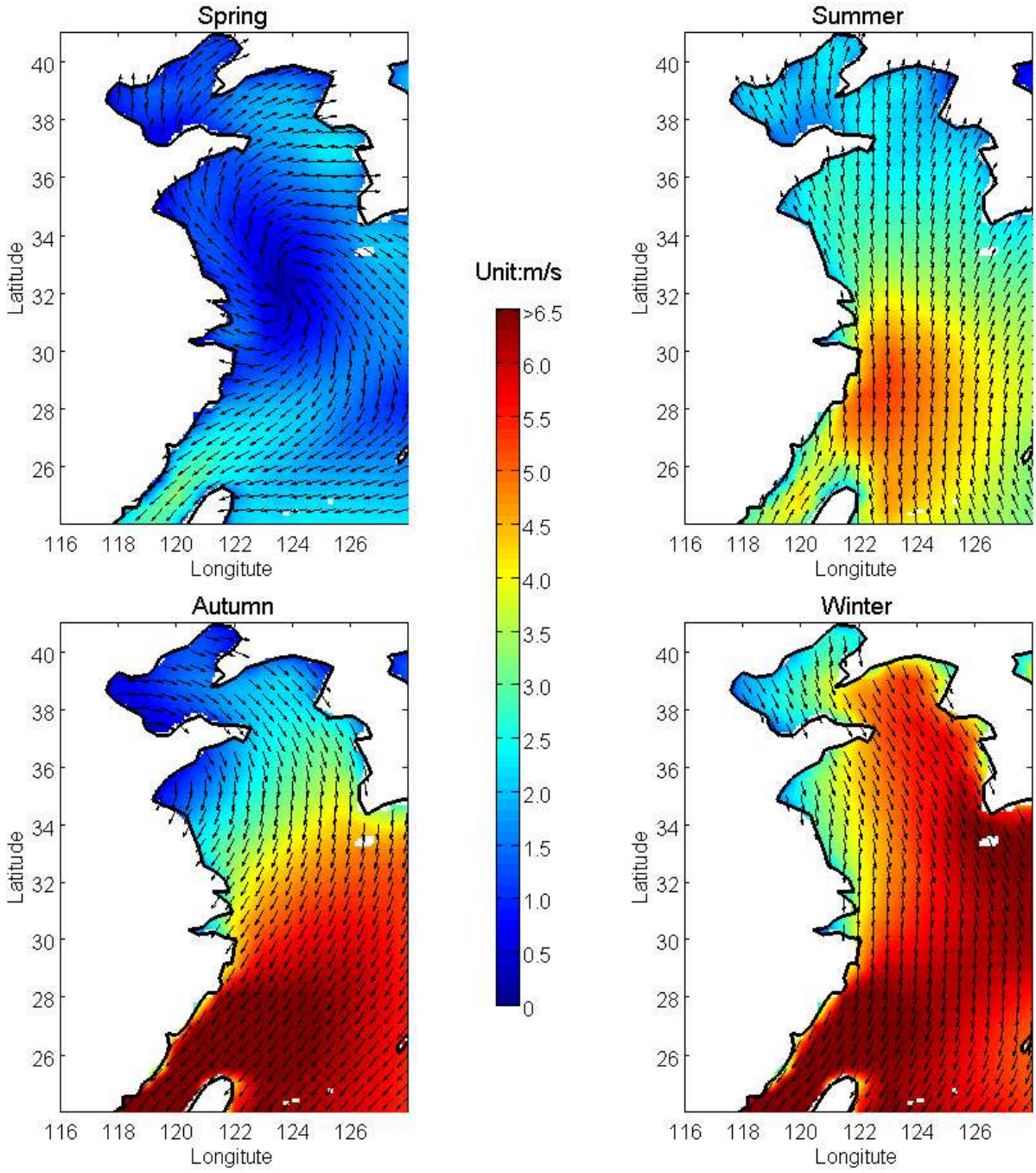

Fig. 6. *Seasonal spatial distribution of the wind vector data in 2003-2013, in which colours indicate wind speed, arrows indicate wind direction, April, July, October and January are the months of spring, summer, autumn and winter.*

3.3. Distribution of Sea Surface 10m Wind over the East China Sea

The each pixel point of the wind vector data over sea surface 10m are averaged according to the latitude and longitude in the same month from 2003 to 2013. The results of wind vector data show the spatial distribution of wind vector from January to December. April, July, October and January are the months of spring, summer, autumn and winter and the seasonal variation were shown in Fig. 6, in which color indicates wind speed, arrows indicate wind direction.

In the spring, the wind speed over the East China Sea was low, the wind direction over Bohai Sea changed from south to southwest with the increasing of longitude. Wind direction over the North Yellow Sea area was WSW. In the South Yellow Sea, wind direction changed from south-eastern in coastal clockwise to west near the shore in the Korean Peninsula, which consistent with the time when Bohai and Yellow Seas appeared cold wave. This anticyclone flow was the average performance of cold anticyclone. In the East China Sea, wind direction over the Taiwan Strait was the northeast, while wind direction was east over the east of the Taiwan island, in the other regions the wind direction

changed from northwest to northeast near the Jeju island, which consistent with the time when the East China Sea appeared cold wave. The change of wind direction reflected the characteristics of cold anticyclone.

In summer, the wind speed increased compared with the spring, the wind direction was the south over the central of the Bohai Sea. The wind direction was the south over the North Yellow Sea beside the coastal waters of Korea Bay whose direction was WSW. In the South Yellow Sea, the wind direction changed from the south-southeast to the southwest with the increasing of longitude. In the East China Sea, the wind direction was the south over the regions of 122ºE~125ºE, and it was southwest in the top of the Taiwan Strait, it is south-southeast over the regions of the east of 125ºE and the south of 26ºE.

In autumn, the wind speed over the Bohai Sea and Yellow Sea was low, and high over the other regions. The wind direction was WNW over Bohai Sea and northwest in North Yellow Sea respectively. The wind direction was south over the South Yellow Sea. In the East China Sea, the wind direction changed from north to northeast with the decrease of latitude.

In winter, cold air from north to south blows off the mainland toward the sea forming the winter monsoon. The wind speed over the East China Sea was higher than the other seasons. The wind direction was NNW over Bohai Sea and North Yellow Sea area. In the South Yellow Sea, the wind direction was north-northwest over the west of the Yellow Sea trough and it was northwest over Yellow Sea trough. In the East China Sea, the wind direction changed from NNW to northeast with the decrease of latitude.

3.4. Relationship Between the Wind Vector and AOD

Over the Bohai Sea and the North Yellow Sea, in spring, the wind direction was southwest, i.e., from the land to the ocean. There was a range of high sandstorm in northern China, which is the main reason for AOD values became the largest and most widely scattered in four seasons. In summer, the wind direction was from the ocean to the land, which forced the sea aerosol to transport outward, therefore the AOD decreased significantly in summer. In autumn, well atmosphere condition leaded to the reduction of the land-basic sources of aerosol and the AOD values over Bohai Sea continued to decrease. The regions with higher AOD values were disappeared. In winter, the spatial distribution of wind direction was similar to the autumn, so the AOD values over the whole Bohai Sea continued to decline significantly.

In the South Yellow Sea, the AOD remained at a high value (0.12-0.14) in spring. In summer, since the wind blew from the East China Sea to the land, the AOD values reduced over the south of the Yellow Sea, while the AOD values grew significantly over the north of the Yellow Sea. The AOD values has increased over the east of Yellow Sea Trough, which may be the reason of the accumulation of aerosol substance, the wind speed over the central of the South Yellow Sea slightly greater than the speed at the junction of the South Yellow Sea and North Yellow Sea. In autumn, although the wind direction over the South Yellow Sea was from the land to the East China Sea, the wind speed over the South Yellow Sea was significantly higher than the North Yellow Sea, the AOD values decreased significantly compared with the summer. In winter, the AOD values increased over the entire west of the Yellow Sea compares with the autumn, which may be relationship between the dust in the land and the wind direction.

The AOD values over the East China Sea were high in the spring, especially in the Taiwan Strait and Okinawa Trough waters, the AOD values appeared a high value about 0.16. In summer, due to the wind direction was from the top of the East China Sea to the land and the wind speed is large, the AOD values over the entire East China Sea show a clear downward trend compared to the spring, especially in the Taiwan Straits, Okinawa Trough reduced significantly. The wind direction in the autumn was from land to the East China Sea, the AOD values over most of the East China Sea showed significant growth trend. In winter, the AOD values over the East China Sea increased clearly and showed an upward trend, especially in the Okinawa Trough waters and Jeju Island, which mainly related to the presence of the dust from the inland in the winter, the pollution of human activity and the wind blow from the land to the East China Sea.

4. Conclusions

The AOD presented obvious annual periodic variation over the East China Sea, the maximum of AOD values appeared in February or March during springtime, while the minimum appeared in autumn. The AOD values increased firstly and decreased in the course of a year, and significant increase from January to March, the maximum of AOD values reached 0.146 and a progressive declined from April to August then it stabilized around 0.1 from September to December. The seasonal changes trend indicated the AOD in spring was slightly higher than in the winter and significantly higher in summer and autumn, in other words the AOD reached the highest value in spring. Spatial and temporal variation of AOD is affected by many factors, especially the monsoon. By analyzed the AOD and wind vector data, there were closely relationship between the AOD and wind field in different sea area near Chinese coast. Overall, the spatial and temporal and distribution and variation of AOD are closely related to the wind direction and speed above the corresponding sea area.

Acknowledgment

The study was supported by Tianjin Natural Science Foundation Project (14JCYBJC22500). The MODIS data used in the present work were obtained from the Ocean Biology Processing Group (OBPG) of the Goddard Space Flight Center (GSFC) in the compressed Hierarchical Data Format (HDF). Wind vector data have been computed using ECMWF reanalysis data. We thank the data distribution centers for their valuable support.

References

[1] An W. J., Pathak R. K., Lee B. H., Pandis S. N., 2007, "Aerosol volatility measurement using an improved thermodenuder: Application to secondary organic aerosol", *Journal of Aerosol Science*, 38, pp. 305-314.

[2] Chen C.-T. A., 2009, "Chemical and physical fronts in the Bohai, Yellow and East China Seas", *Journal of Marine Systems*, 78, pp.394–410.

[3] Chudnovsky A. A., Koutrakis P., Kloog I., Melly S., Nordio F., Lyapustin A., Wang Y. J., Schwartz J., 2014, "Fine particulate matter predictions using high resolution.

[4] Aerosol Optical Depth (AOD) retrievals", *Atmospheric Environment*, 89, pp. 189-198.

[5] Cong Z. Y., Kang S. C., Liu X. D., Wang G. F., 2007, "Elemental composition of aerosol in the Nam Co region, Tibetan Plateau, during summer monsoon season", *Atmospheric Environment*, 41, pp. 1180-1187.

[6] Cong Z. Y., Kang S. C., Smirnov A., Holben B., 2009, "Aerosol optical properties at Nam Co, a remote site in central Tibetan Plateau", *Atmospheric Research*, 92, pp. 42-48.

[7] Fraser R. S., Kaufman Y. J., Mahoney R. L., 1984, "Satellite measurement of aerosol mass and transport", *Atmospheric Environment*,18, pp. 2577-2584.

[8] Glantz P., Nilsson E. D., Hoyningen-Huene W. von, 2009, "Estimating a relationship between aerosol optical thickness and surface wind speed over the ocean", *Atmospheric Research*, 92, pp. 58-68.

[9] Guo J. P., Zhang X. Y., Wu Y. R., Zhaxi Y. Z., Che H. Z., La B., Wang W., Li X. W., 2011, "Spatio-temporal variation trends of satellite-based aerosol optical depth in China during 1980-2008", *Atmospheric Environment*, 45, pp. 6802-6811.

[10] Lee J., Kim J., Lee Y. G., 2014, "Simultaneous retrieval of aerosol properties and clear-sky direct radiative effect over the global ocean from MODIS", *Atmospheric Environment*, 92, pp. 309-317.

[11] Lee S., Ghim Y. S., Kim S. W., Yoon S. C., 2009, "Seasonal characteristics of chemically apportioned aerosol optical properties at Seoul and Gosan, Korea", *Atmospheric Environment*, 43, pp. 1320-1328.

[12] Li Y. J., Xue Y., Leeuw Gerrit de, Li C., Yang L. K., Hou T. T., Marir F., 2013, "Retrieval of aerosol optical depth and surface reflectance over land from NOAA AVHRR data", *Remote Sensing of environment*, 133, pp. 1-20.

[13] Luo N. N., Wong M. S., Zhao W. J., Yan X., Xiao F., 2015, "Improved aerosol retrieval algorithm using Landsat images and its application for PM_{10} monitoring over urban areas", *Atmospheric Research*, 153, pp. 264–275.

[14] Mehta M., 2015, "A study of aerosol optical depth variations over the Indian region using thirteen years (2001–2013) of MODIS and MISR Level 3 data", *Atmospheric Environment*, 109, pp. 161-170.

[15] Meij A.de, Pozzer A., Lelieveld J., 2012, "Trend analysis in aerosol optical depths and pollutant emission estimates between 2000 and 2009", *Atmospheric Environment*, 51, pp. 75-85.

[16] Moula M., Verdebout J., Eva H., 2002, "Aerosol optical thickness retrieval over the Atlantic Ocean using GOES imager data", *Physics and Chemistry of the Earth*, 27, pp. 1525-1531.

[17] Stopa J. E., Cheung K. F., 2014, "Intercomparison of Wind and Wave Data from the ECMWF Reanalysis Interim and the NCEP Climate Forecast System Reanalysis", *Ocean Modelling*, 75, pp. 65-83.

[18] Sun X. P, 2008, Coastal Regional Oceanography in China, Beijing: Ocean Press.

[19] Sundström A. M., Kolmonen Sogacheva P., L., Leeuw G. de, 2012, "Aerosol retrievals over China with the AATSR dual view algorithm", *Remote Sensing of Environment*, 116, pp. 189-198.

[20] Tai A. P. K., Mickley L. J., Jacob D. J., 2010, "Correlations between fine particulate matter ($PM_{2.5}$) and meteorological variables in the United States: implications for the sensitivity of $PM_{2.5}$ to climate change", *Atmospheric Environment*, 44, pp. 3976-3984.

[21] Wang J., Xu X. G., Spurr R., Wang Y. X., Drury E., 2010, "Improved algorithm for MODIS satellite retrievals of aerosol optical thickness over land in dusty atmosphere: Implications for air quality monitoring in China", *Remote Sensing of Environment*, 114, pp. 2575-2583.

[22] Wei. F. Y., 2007, Modern diagnosis and prediction of climate statistics, Meteorological Press. Beijing, 2nd edition.

[23] Yuan Y., Shuai Y., Li X. W., Liu B., Tan H. P., 2014, "Using a new aerosol relative optical thickness concept to identify aerosol particle species", *Atmospheric Research*, 150, pp. 1-11.